

# The Influence of Diffusion- and Relaxation-Related Factors on Signal Intensity: An Introductory Guide to Magnetic Resonance Diffusion-Weighted Imaging Studies

Stefano Colagrande, MD,\* Giacomo Belli, MS,† Letterio Salvatore Politi, MD,‡  
Lorenzo Mannelli, MD,\* Filippo Pasquinelli, MD,\* and Natale Villari, MD\*

**Abstract:** In magnetic resonance diffusion-weighted imaging, signal intensity is influenced simultaneously by temperature, diffusivity, b value, pseudodiffusion, macroscopic motion, and T2-weighted intensity value. The purpose of this pictorial essay is to discuss and exemplify the influence that such factors and the related modifications have on signal intensity. Apparent diffusion coefficient, shine-through and pseudodiffusion will also be examined to show how T2-weighted signal intensity value and nondiffusional intravoxel incoherent motion can affect the diffusion-weighted imaging.

**Key Words:** diffusion-weighted imaging, apparent diffusion coefficient, shine-through effect, pseudodiffusion, intravoxel incoherent motion, lack of mobile spin effect

(*J Comput Assist Tomogr* 2008;32:463–474)

Magnetic resonance (MR) diffusion-weighted imaging (DWI) allows measuring the degree of diffusion of water molecules in biological tissues *in vivo*. However, several diffusivity-related factors can influence diffusion-weighted (DW) signal intensity (SI) and should be taken into consideration for an accurate interpretation of resultant images.

The diffusivity-related factors such as b value, temperature, diffusivity, pseudodiffusion, macroscopic motion, and T2-weighted SI value are of common knowledge, but as far as we know, they have never been collectively explained, mathematically described, nor interrelated using *in vitro/in vivo* illustrative examples. The purpose of this review is to discuss and illustrate the influence that such factors and related modifications have on SI.

Our data were acquired with a 1.5-T superconducting MR body scanner (Intera 10.2; Philips Medical Systems, Eindhoven, The Netherlands), equipped with high-

performance gradients (maximum strength of 30 mT/m; maximum slew rate of 150 mT/m per millisecond). Sequence parameters will be described in captions. To optimize signal-to-noise ratio, a 4-element quadrature phased-array surface coil was used. The diffusion gradients were applied in 3 orthogonal directions: frequency-encoding (*x*), phase-encoding (*y*), and slice-selection directions (*z*). Finally, to reduce chemical shift artifacts, frequency-selective fat saturation was used in all *in vivo* diffusion acquisitions.

## DIFFUSIVITY, DIFFUSION, AND APPARENT DIFFUSION COEFFICIENT

Diffusion is the inconsistent and random microscopic motion of water molecules, caused by thermal energy and known as Brownian motion. In a liquid solution, the self-diffusion of the water molecules strictly depends on the temperature and the viscosity of the solution: the greater the temperature the wider the molecular random movements.

To demonstrate how the self-diffusivity of the water molecules is influenced by the thermal energy, we devised an experiment in which we measured the diffusion coefficient of an adequate quantity of water, filling 3 test tubes, and held at 3 different temperatures (Fig. 1). The plastic test tubes thermal insulation was ensured by a polystyrene foam envelope. With the aim to verify any thermal change, the temperature of water in each tube was measured by a digital thermometer, either just before the beginning or immediately after the conclusion of the acquisition sequence.

Diffusion can be studied and measured by MR using an appropriately designed turbo spin-echo or echo-planar sequence with 2 complementary dephasing-rephasing gradients. Spins accumulate a phase change depending on their position with respect to the first field gradient. A second imposed gradient, equal and opposite to the previous, induces a complete rephasing in the stationary spins and an incomplete rephasing in the mobile spins.<sup>1,2</sup> As a consequence, the motion of the mobile spins between the 2 complementary opposite gradients causes a signal loss that is proportional to the entity of the spin drift: the greater the displacement of the spins, the greater the loss of signal in relation to that produced by the same stationary spins. Strength, temporal spacing, and duration of the 2 motion probing gradients are expressed by the sensitization factor b

From the \*Department of Clinical Physiopathology, Section of Radiodiagnos-  
tics, University of Florence, Azienda Ospedaliero-Universitaria Careggi;  
†Department of Medical Physics, Azienda Ospedaliero-Universitaria  
Careggi; and ‡Department of Neuroradiology, San Raffaele Scientific  
Institute, Milan, Italy.

Received for publication February 27, 2007; accepted May 16, 2007.

Reprints: Stefano Colagrande, MD, Sezione di Radiodiagnostica, Diparti-  
mento di Fisiopatologia Clinica, Università degli Studi di Firenze,  
Azienda Ospedaliero-Universitaria Careggi, Viale Morgagni 85, Firenze,  
Italy 50134 (e-mail: stefano.colagrande@unifi.it).

Copyright © 2008 by Lippincott Williams & Wilkins

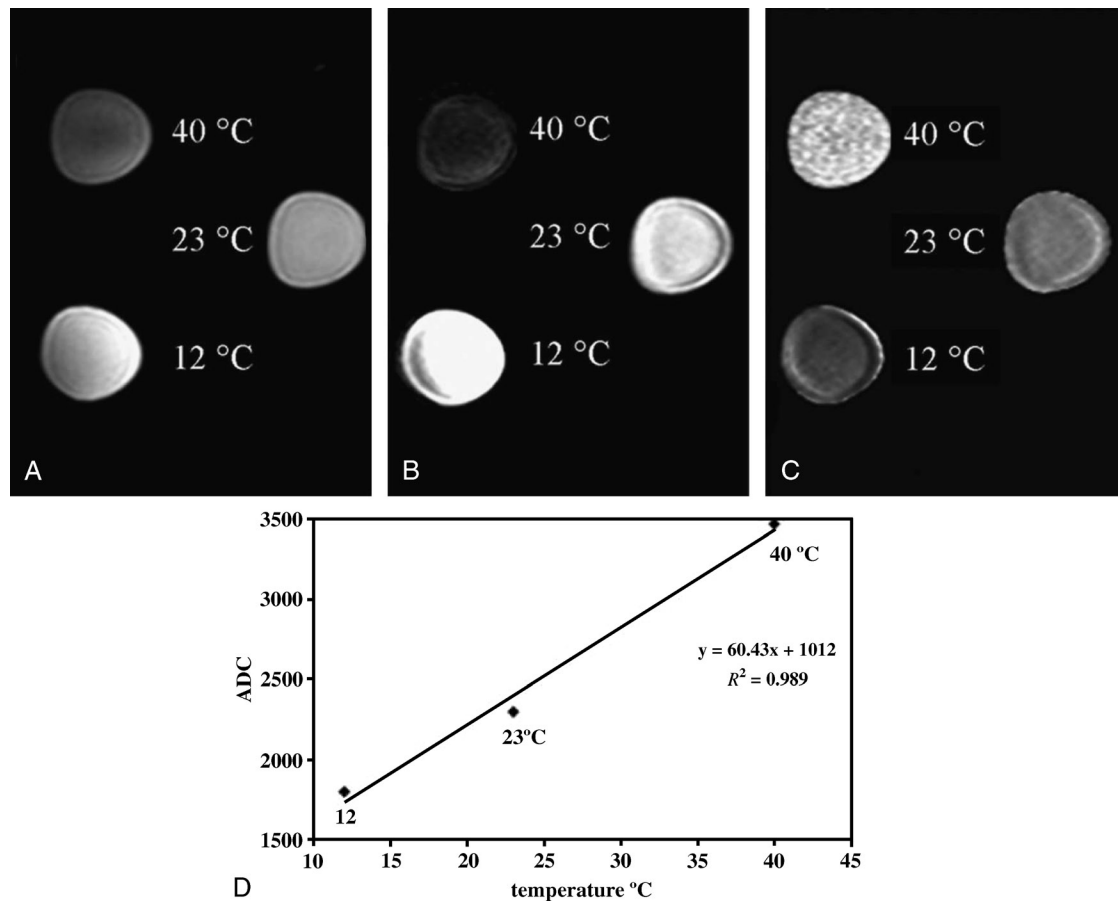


**FIGURE 1.** Phantom and related graph: temperature effect on water-free diffusion. Diffusion-weighted single-shot echo-planar MR images (repetition time/echo time, 1900/74), b values 0 s/mm<sup>2</sup> (A) and 600 s/mm<sup>2</sup> (B), and corresponding ADC map (C) of 3 test tubes, filled with water held at 3 different temperatures: upper left, 40°C; center right, 23°C; lower left, 12°C. The plastic test tubes thermal insulation was ensured by a polystyrene foam envelope. The mobility of the water molecules depends on thermal energy: the higher the temperature of water, the broader the Brownian motion, the lower the SI in DWI and the higher the ADC. The ADC of the 3 water samples is plotted (y axis) versus temperature (x axis): the graph (D) demonstrates an approximately linear dependence of the diffusion coefficient on the temperature, which ranges from 12°C to 40°C. As shown, the linear dependence is demonstrated by the high coefficient of correlation ( $R^2 = 0.989$ ). The SI differences among the test tubes at b value 0, is caused both by effect of imaging alternating gradients and temperature variation. In fact, the latter links with the correlation time and then, as stated by Solomon-Bloembergen theory, with relaxation rates. In a nonviscous liquid like the water, when temperature increases, correlation time decreases, and both T1/T2 become longer. The slight decrement of the SI showed by the water in the test tube (b = 0) when temperature increases (from 12°C to 40°C) is then determined by the T1 lengthening, as well.

(s/mm<sup>2</sup>). Stated in general, as b increases, so does the real diffusion weighting of the sequence. Diffusion of water spins, therefore, always produces a signal loss, whereas in the case of reduction in diffusivity, a relative regional preservation in SI can be observed (Fig. 2). The SI obtained with a diffusion-weighting sequence varies with the ability of water molecules to diffuse randomly in relation to their chemical interactions and with the structural components of the tissues (ratio of the water bonded to the macromolecules, mainly proteins) (Fig. 3). To further explain the diffusive phenomena, we refer to the observation of various test tubes filled with water and increasing concentration of sucrose (Fig. 4). As shown, in phantom test tubes, the higher is the percentage of sucrose in the sample, the lower

is the diffusivity, and the higher is the SI in DWI. Sucrose molecules reduce the motion of water molecules with a consequent SI increase in DWI. Taking into account the random movement of water molecules, the SI loss, with respect to the signal intensity  $SI_0$  obtained with the gradient strength b switched off, can be expressed by the equations

$$SI = SI_0 \cdot \exp(-b \cdot ADC) \quad (1)$$

$$ADC = 1/b \cdot \ln(SI_0/SI) \quad (2)$$

in which the factor ADC is the apparent diffusion coefficient: the higher the value of ADC and/or b factor, the stronger the loss of SI.

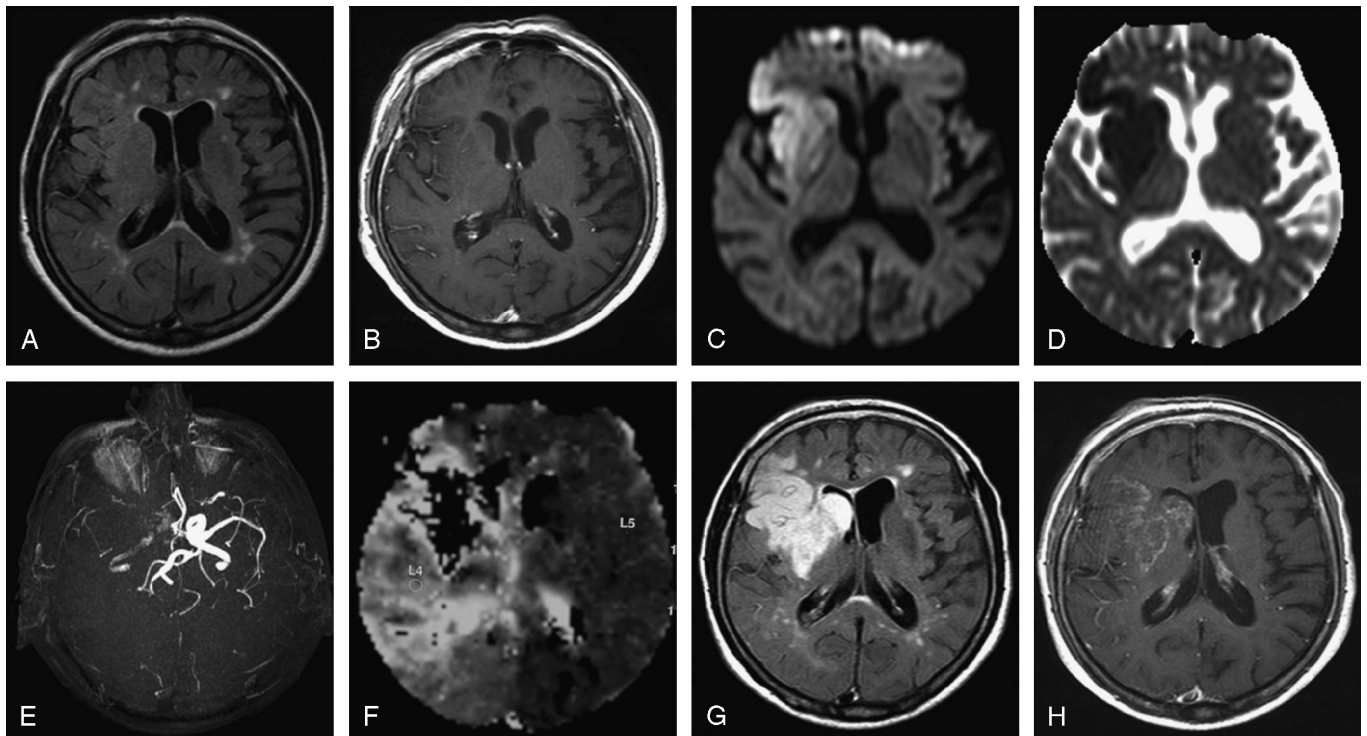


**FIGURE 2.** A 81-year-old woman with hyper acute stroke: true diffusion reduction and correlated SI. Axial fluid attenuated inversion recovery (FLAIR) (repetition time/echo time, 11000/120; inversion time, 2200) (A) and contrast-enhanced spin-echo T1-weighted (600/15) (B) MR images obtained 4 hours after the onset of left hemiparesis. Only in the FLAIR image, a slight SI alteration in the right cortical frontal and insular regions can be noticed. Axial single-shot echo-planar DW MR image (3570/120), b value 1000 s/mm<sup>2</sup> (C), and corresponding map (D) acquired during the same MR examination clearly demonstrate a broad area of restricted diffusion (hyperintense and hypointense, respectively) in the right corticosubcortical frontal and insular region, and lenticular and caudate nuclei. Maximum intensity projection of 3-dimensional time of flight MR angiography (E) and mean transit time perfusion map (F) obtained at that time document occlusion of the right internal carotid artery and a broad area of ischemic penumbra, respectively. Axial FLAIR (11000/120) (G) and contrast-enhanced spin-echo T1-weighted (600/15) (H) MR images acquired 24 hours after the onset, reveal the ischemic lesion which becomes clearly evident also in conventional MR sequences. In the FLAIR acquisition (G), the high quantity of free water because of coexistence of cytotoxic and vasogenic edema well explains the SI of the lesion. Subtle dysfunction of the blood-brain barrier accounts for the faint contrast enhancement (H).

In biological tissues, microscopic motion detected by DWI includes both diffusion of water molecules, influenced by the structural components of the tissue, and microcirculation of blood in the capillary network (perfusion).<sup>3,5</sup> Moreover, molecular motion owing to concentration gradients cannot be differentiated from molecular activity because of pressure, thermal gradients, or ionic interactions.

When the perfusion contribution is negligible, ADC coincides with the diffusion coefficient *D* in homogenous and isotropic media because it describes the molecular average motion in an overall direction. Thus, ADC can only partially describe a more composite event when the media is anisotropic. In the case of anisotropic structures, the diffusion coefficient changes, with the variation of the orientation of the diffusion gradient with respect to the direction of the fibers, as seen in the example of the white matter tracts in the central nervous system (Fig. 5).

Apparent diffusion coefficient, expressed as a scalar quantity, is unable to fully describe diffusion in anisotropic media. In the latter case, a full mathematical description is

exclusively made possible by a tensor, which is an operator capable of taking into consideration the correlations between the 3 orthogonal directions. Although this point and the related mathematical descriptions are not the subject of the present paper, detailed explanations can be found in published sources.<sup>2,7,8</sup>

An average diffusivity image, known as *trace* or *isotropic*, can be obtained from the images related to each one of the orthogonal gradient directions (frequency encoding, phase encoding, and slice selection) of the diffusion (Fig. 5).

## T2 EFFECTS ON DW SI

The long repetition times and echo times which enable the activation of the complementary dephasing/rephasing gradients, also produce DW images that are heavily weighted on T2. The so-called *T2 shine-through* phenomenon is a typical example of how the T2-weighted SI can affect the DW images, in particular those with low b value. In fact, the *T2 shine-through* effect decreases when the b value increases (Fig. 6).

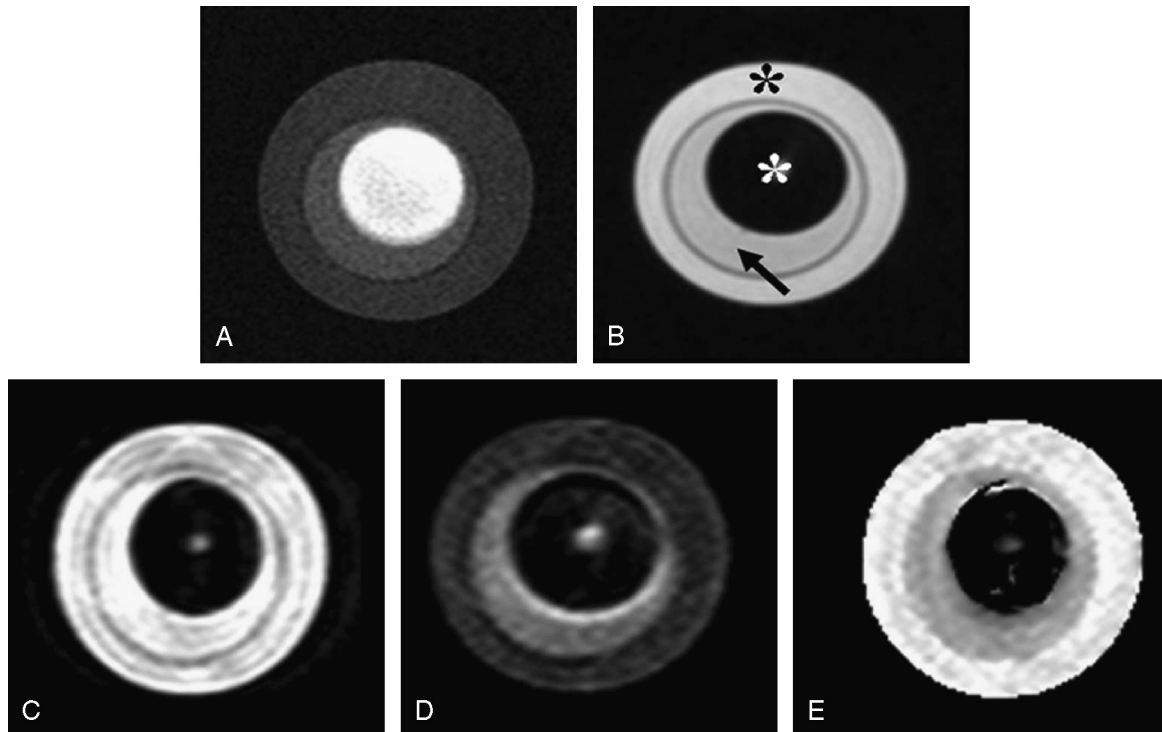


**FIGURE 3.** Phantom: amount of free water and proteins, diffusivity, and correlated SI. Spin-echo T1-weighted (repetition time/echo time, 325/15) (A), turbo spin-echo T2-weighted (3030/100) (B), turbo spin-echo DW MR images (1000/96), b values 0 (C) and 600 s/mm<sup>2</sup> (D), and corresponding ADC maps (E) of a chicken egg surrounded by water (black asterisk). The albumin (black arrow) of the egg appears with lower SI in T1 and with higher SI in T2 and DWI, and b value 0 s/mm<sup>2</sup> (T2 equivalent) sequences, whereas the opposite is seen for the yolk (white asterisk). Diffusivity of egg white is lower than water because of the amount of proteins. The egg yolk appears dark in both (b = 0 s/mm<sup>2</sup> and b = 600 s/mm<sup>2</sup>) DW images and in ADC map, demonstrating an absence of free-water diffusible substrate (lack of mobile spin effect).

Owing to this phenomenon, even in regions where diffusivity is expected to be high (low SI in DWI), SI on DW images may yield high results as a consequence of the long T2 of unbound water. This T2 effect on SI can be noticed, for example, in a cystic lesion in which movement of water molecules is free (Fig. 7).

Therefore, at low b value, high SI on DWI may be caused either by reduced diffusion (Figs. 2, 4) or by T2 shine-through effect, as in the liquid-cystic content (Figs. 6, 7).<sup>6,7,9</sup>

From the mathematical point of view, the effect of T2 on SI is described by the equation

$$SI_0 = SM \cdot \exp(-TE/T2) \quad (3)$$

where SM is the signal maximum amplitude available that depends on T1 and proton density.

If we substitute the equation 1 into the equation 3, we obtain

$$SI = SM \cdot \exp(-TE/T2) \cdot \exp(-b \cdot ADC). \quad (4)$$

From the latter equation 4, we can understand that the effect of T2-weighted SI [ $\exp(-TE/T2)$ ] could be limited by using shorter echo times with stronger diffusion-sensitizing gradient b.

However, as expected from the attenuation factor [ $\exp(-b \cdot ADC)$ ] present in equation 4, SI is more sensitive to b

values in the case of tissues with an attenuation factor close to 1 (that is,  $b \cdot ADC \approx 1$ ). As a matter of fact, in tissues where  $b \cdot ADC \approx 1$ , an increment of the b value from 500 s/mm<sup>2</sup> to 1000 s/mm<sup>2</sup> will result in a SI reduction of about of 74%. Conversely, when  $b \cdot ADC \approx 0.5$ , an identical b value variation from 500 s/mm<sup>2</sup> to 1000 s/mm<sup>2</sup> will determine a SI reduction approximately of 40%.

On the contrary, a low SI on DWI can be determined by 2 different conditions: high tissue diffusivity or short T2. The short T2 effect is caused by a decrease or an absence of free-water molecules sometimes called the *washout* phenomenon (to the best of our knowledge, no references of this term can be found in the indexed literature). Nevertheless, the term *washout* is not very descriptive for this phenomenon because spins are not physically washing out of any slice or voxel. Rather, it is caused by a reduction of the diffusible substrate, and thus, we can call it *lack of mobile spin* effect. This phenomenon can be observed in the case of egg yolks (Fig. 3), in liver coagulation (dehydrated) necrosis post percutaneous ablative treatment (Fig. 8) and in fibrotic tissue.

It should be underlined that T2 shine-through and, more in general, T2-weighted related effects are always present in DW images, even if these effects can be reduced by increasing the b value.

To clear out T2-weighted effects in DWI, ADC maps should be calculated. In contrast to the DW images, ADC maps are not influenced by the effects of T2-weighted. In fact, because the term T2 is contained in both  $SI_0$  and SI, if we substitute the equation 3 with the equation 2, we obtain.

$$\frac{1}{b} \cdot \ln\left\{\frac{SM \cdot \exp(-TE/T_2)}{SM \cdot \exp(-TE/T_2)} \cdot \exp(-b \cdot ADC)\right\}$$

and then, after simplification (underlined terms)

$$\frac{1}{b} \cdot \ln\left\{\frac{SM}{SM \cdot \exp(-b \cdot ADC)}\right\} \equiv ADC \quad (5)$$

In the identity expression 5, it is evident that the dependence on T2 is canceled. In ADC maps, hyperintensity indicates high diffusivity, whereas hypointensity represents low diffusivity. Apparent diffusion coefficient maps, therefore, show a direct correlation with the entity of diffusivity.

### PSEUDODIFFUSION AND MACROSCOPIC MOTION EFFECTS ON DW SI

Apparent diffusion coefficient is an artificial parameter and its value represents all the intravoxel incoherent motion (IVIM). In fact, ADC incorporates not only diffusion motions but also the so-called pseudodiffusion ( $D^*$ ) that consists of motions derived from perfusion.<sup>5,7,10</sup> Thus, ADC values also depend on SI alterations deriving from  $D^*$  and consequently are equal to the real diffusion D only when the latter is the sole motion. Moreover, ADC is influenced by bulk, macroscopic motions, as well.

As a consequence, due to perfusion, ADC has a higher value in living tissues than otherwise expected, as already discussed. This phenomenon can be easily demonstrated in DWI acquisitions of the upper abdomen (Fig. 9), being the ADC value of a living tissue also dependent from perfusional IVIM ( $D^*$ ), it relies on b value, as well. In particular, as shown in (Fig. 9G) and explained by the following mathematical functions,  $D^*$  dependence is

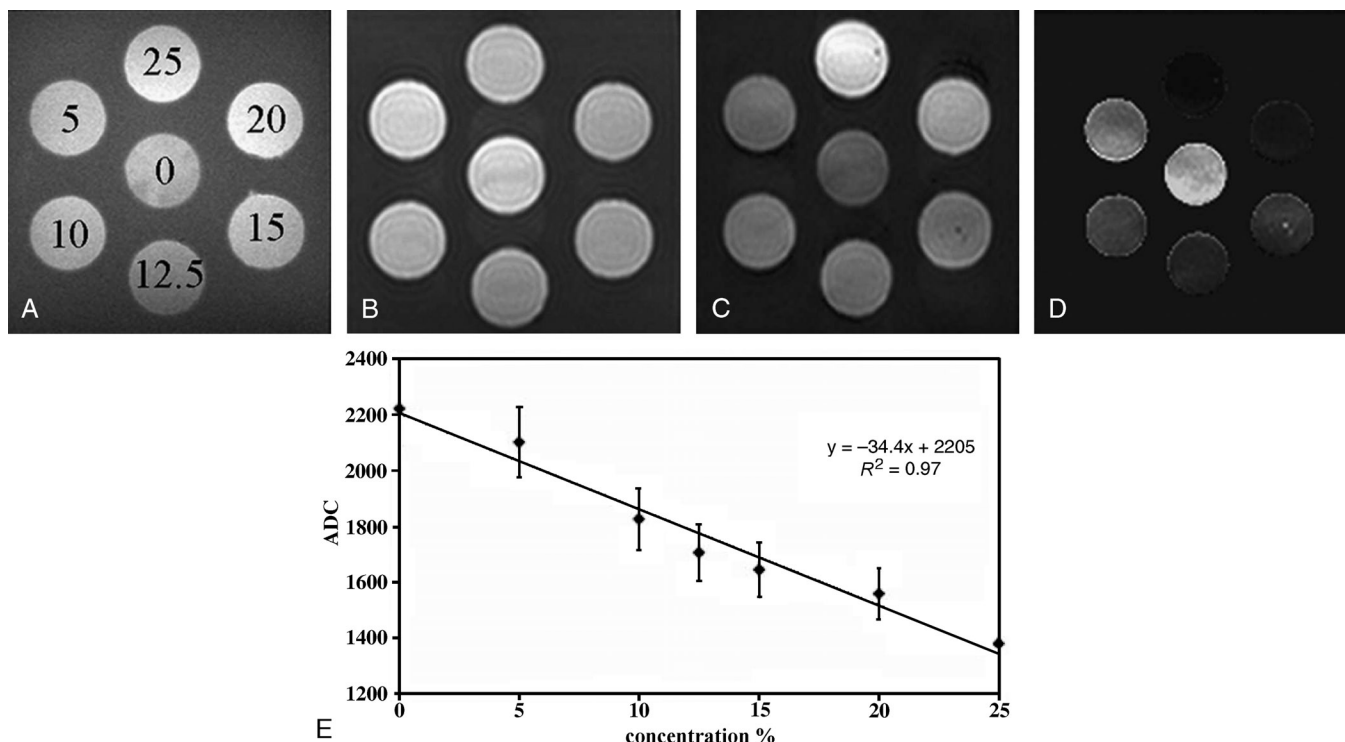


**FIGURE 4.** Phantom and related graph: concentration effect on water-free diffusion. Spin-echo T1-weighted (repetition time/echo time, 160/15) (A), turbo spin-echo DW MR images (3000/140), b values 0 (B) and 1000 s/mm<sup>2</sup> (C), and corresponding ADC map (D) of a phantom, made of agarose gel (1%) with 7 hollow cylinders filled with a liquid solution at different percent weight sucrose per weight water (0%, 5%, 10%, 12.5%, 15%, 20%, 25%). The experiment demonstrates the dependence of free diffusive phenomena of the water molecules on sucrose concentration: the higher the concentration, the lower the diffusivity phenomena, the higher the SI in DW image (b = 1000 s/mm<sup>2</sup>) and the lower ADC value in the map. Signal intensity in T1-weighted image is high, due to a small amount of a much-diluted paramagnetic salt, stirred into the solution to provide for less signal saturation. The ADC (in 10<sup>-6</sup> mm<sup>2</sup>/s unit) of 7 different concentrations of a liquid solution with water and sucrose (y axis) is plotted versus the concentration value (x axis) (E). A regression line is drawn through the experimental points. The ADC of the pure water is slightly lower than the expected value (2300 10<sup>-6</sup> mm<sup>2</sup>/s) which can be explained by the small amount of paramagnetic salt that was added to reduce saturation effects. As shown, the inverse linear dependence is demonstrated by the high coefficient of correlation ( $R^2 = 0.97$ ).

lowered by high  $b$  value, which simultaneously increases weighting in  $D$ .

From the mathematical point of view, the effect of the perfusion on the total SI can be modeled by taking into account the volume fraction  $f$  of the tissue water flowing through the microvessels. Consequently, the spin-echo attenuation relation 1 will have to include an additional term accounting for magnetization dephasing because of microcirculation and mimicking a diffusion process. Hence, the signal loss is described by a biexponential function versus  $b$ :

$$SI = SI_0 \cdot \exp(-b \cdot D)(1-f) + f \cdot \exp(-b \cdot D^*), \quad (6)$$

where  $D$  is the true-water diffusion coefficient, whereas  $D^*$ , called pseudodiffusion coefficient, accounts for the perfusion flow.<sup>1</sup> To separate the different effects ( $D$  and  $D^*$ ), a sequence with several values of the sensitizing diffusion factor  $b$  should be planned.

Then, by applying the equation 2 over the relation 6, we obtain an expression for ADC that depends on the values of  $D$  and  $D^*$  in a quite complex manner:

$$ADC = D - 1/b \cdot \ln\{[1-f \cdot (1-\exp(-b \cdot D^*))]\}. \quad (7)$$

Such equation can be simplified, making some approximate transformations for the exponential and the logarithmic terms, according to the following practical hypothesis:

1. for weak diffusion gradients or  $D^*$  small enough so that  $b \cdot D^* \ll 1$  and

$$ADC \approx D + f \cdot D^* \quad (7a)$$

2. for a small perfusion fraction:  $f \ll 1$  and for diffusion gradients strong enough so that  $b \cdot D^* \gg 1$

$$ADC \approx D + f/b. \quad (7b)$$

From equation 7b, we can deduce that, when the  $b$  factor is high, the ADC value will result closer to the true

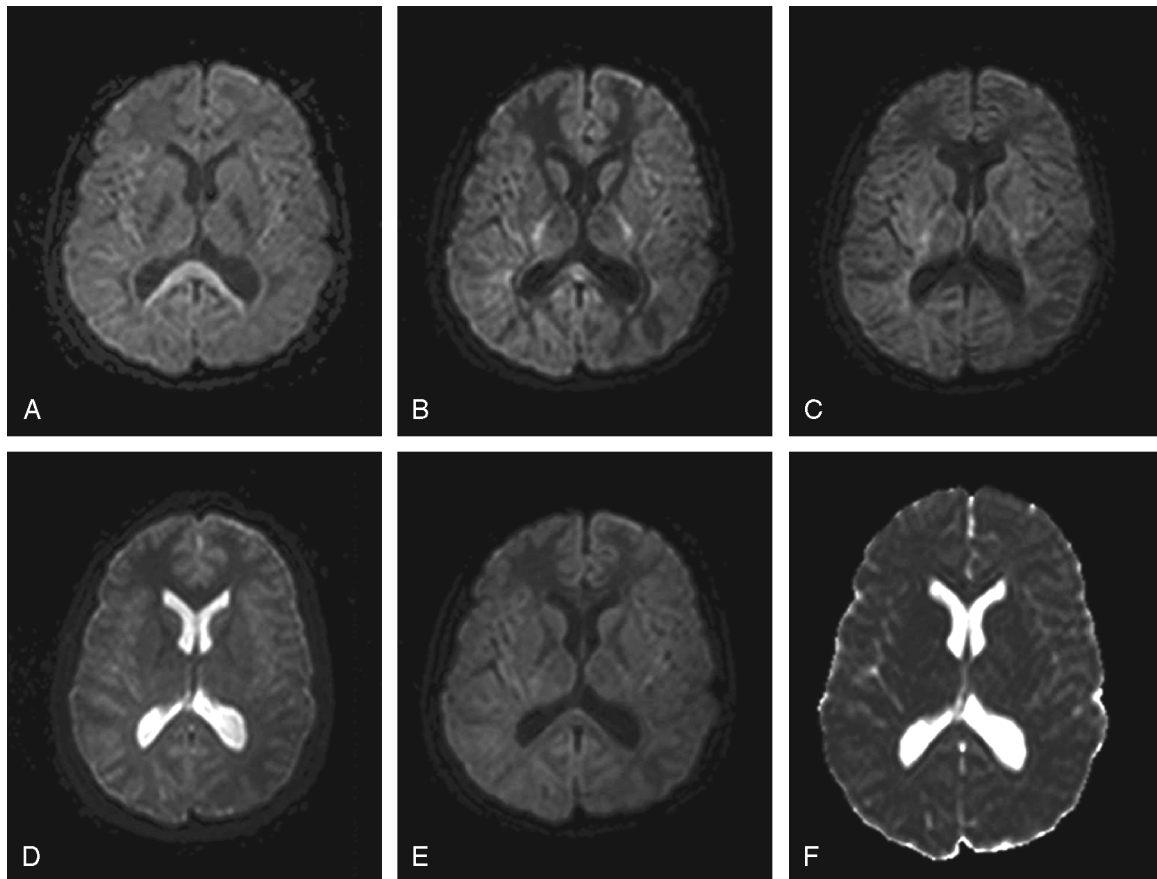


**FIGURE 5.** A 27-year-old man with normal brain: anisotropy and diffusivity variation with the orientation of the sensitization gradient. Axial single-shot echo-planar DW MR image (repetition time/echo time, 3570/120),  $b$  value 1000  $s/mm^2$  with diffusion gradients applied along slice selection ( $s$ ) (A), phase encoding ( $p$ ) (B), and readout ( $m$ ) direction (C) shows different SI of the white matter tracts, depending on the different orientation of the applied sensitization gradient. Axial single-shot echo-planar DW MR isotropic (trace) image (3570/120),  $b$  values 0 (D) and 1000  $s/mm^2$  (E), and corresponding ADC map (F). Isotropic image, from the mathematical point of view, is the cube root of the product of the other 3 diffusion images relative to  $s$ ,  $p$ , and  $m$ . The ADC map value calculated on this isotropic image is independent from the phenomenon of anisotropism and is adopted as a first approximation to estimate the mean diffusivity of the sample.

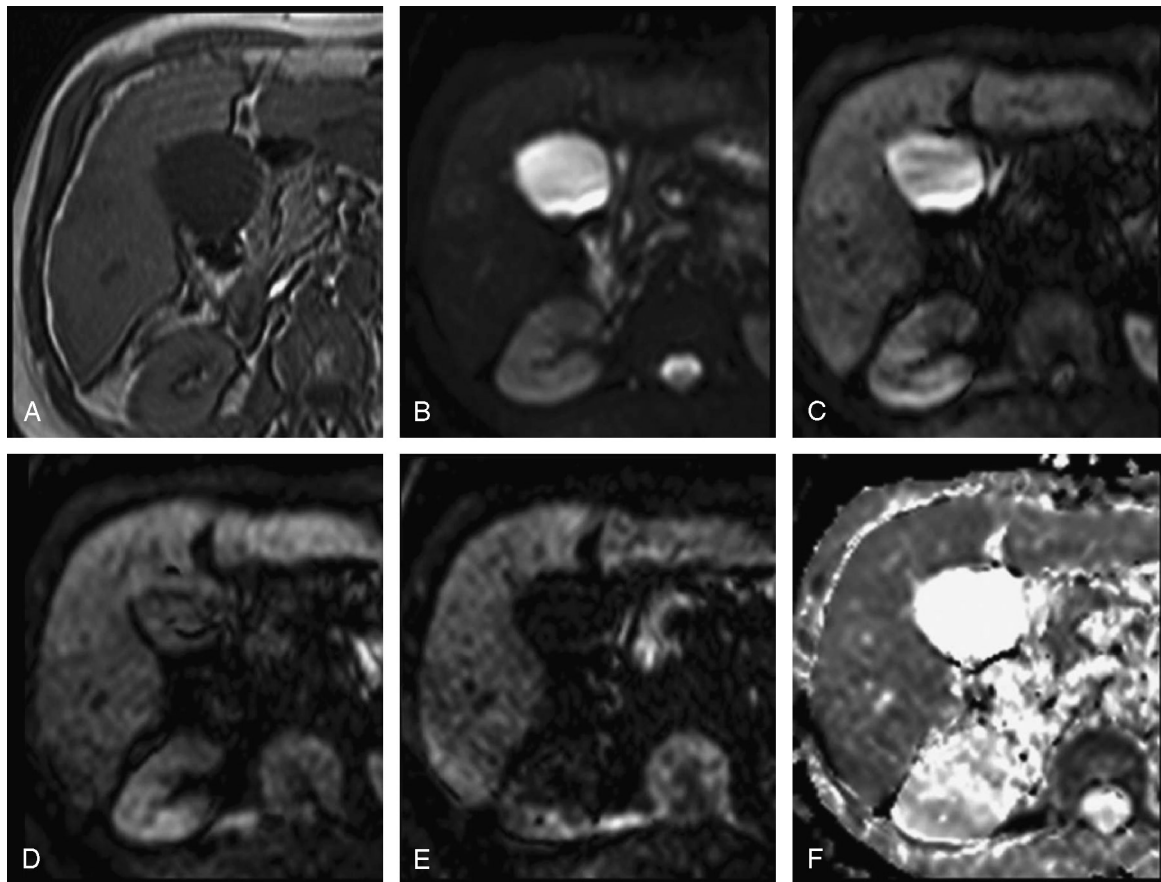


**FIGURE 6.** A 68-year-old man with normal liver and gallbladder: shine-through effect. Axial gradient-echo T1-weighted (repetition time/echo time, 146/2) (A), axial single-shot echo-planar DW MR images (1900/74), b values 0 s/mm<sup>2</sup> (B), 333 s/mm<sup>2</sup> (C), 667 s/mm<sup>2</sup> (D), and 1000 s/mm<sup>2</sup> (E), and corresponding ADC map (F). Diffusion-weighted images demonstrate how gallbladder SI lessens with the increment of the b factor value. At low b value, the SI of the bile results higher than expected because of shine-through effect. When b increases, shine-through effect decreases. Corresponding ADC map shows elevated SI because of high bile diffusivity.

diffusion coefficient. Thereby, for large b values, the pseudodiffusion effects are lowered, and the dependence of ADC from the perfusion decreases.

As a matter of fact, in a liquid substance also, the bulk motion of molecules can be often overlapped to the natural diffusion process. In DW sequences, the nonperfect rephasing of mobile magnetizations causes a signal loss that does not follow an exponential function. The attenuation of the SI depends on the b value, on the mean velocity of the macroscopic motion, and on the angle between the direction of the motion and the field gradient direction, as well.

Examples of such bulk, macroscopic movements which can contaminate DWI studies are represented by other nondiffusional macroscopic motions as cardiovascular, respiratory, and peristaltic movements.

With the purpose of explaining the role of a nonspecific macroscopic motion on DWI, we can perform a simple experiment (Fig. 10) using as additional movement the cerebrospinal fluid (CSF) pulsation. Such physiological motion and its related changes in 2 different

pathological conditions (ie, normotensive hydrocephalus and obstructive hydrocephalus) allows for a visual assessment of the effects of a supplementary macroscopic motion to the true diffusion.

By placing a test tube containing saline solution next to the head of a patient affected by normotensive hydrocephalus, DW sequences with low b values may show that the SI in ventricles and in the test tube differs, even if both contain free diffusible water molecules. In the test tube, DWI SI is higher than in ventricles. The different temperature (22°C) at which the test tube is held with respect to ventricles (37°C) does not entirely explain this strong SI difference, especially for low b value. By increasing the b value from 150 to 1200 s/mm<sup>2</sup> (Fig. 10), the difference in SI between the saline solution and CSF progressively decreases, without annulling.

For b values lower than b equals to 1200 s/mm<sup>2</sup>, CSF shows ADC values higher than those measured in the test tube, varying nonlinearly for different b factors. Such difference in ADC values is not well accounted for the simple difference of temperature.

This divergence can be explained by CSF flow. In fact, in the test tube solution, there is no additional water dislocation due to CSF flow. In the ventricles, the ADC value depends on the sum of diffusion (D) of CSF (roughly similar to that of the saline solution) plus a term due to the attenuation of the signal determined by CSF flow. By increasing the b value, we can observe a reduction of motion effects regardless of the cause. On the contrary, when CSF flow decreases, as in obstructive hydrocephalus (Fig. 11), the motion effects result less significant and DWI SI increases, if all other parameters are kept stable.

Finally, at high b values ( $b = 1200 \text{ s/mm}^2$ ), the CSF flow effect becomes almost negligible, and the higher ADC of CSF with respect to saline solution is explained by the different temperatures ( $37^\circ$  and  $22^\circ$ , respectively) (Figs. 1, 12).

In the given example, for low b factor, macroscopic motion markedly influences the obtained values of ADC, whereas a high b factor makes less important, even if not

always negligible, the influence of the motion on the signal decay because of the true diffusion effect (Fig. 12).

## CONCLUSIONS

In DWI, SI is mainly influenced by diffusivity, pseudodiffusion, macroscopic motion, and T2-weighted intensity value; the latter is to be considered as an index of the amount of free-water molecules in the examined voxel. Apparent diffusion coefficient is a scalar quantitative parameter insensitive to T2 effects and incorporating all the IVIM. To obtain an image which is truly representative of diffusivity, a high b value is required, and ADC maps should be calculated. In fact, high b values increase the *weighting* in D and determine a progressive reduction of T2, pseudodiffusion, and macroscopic motion effects. Apparent diffusion coefficient mapping, instead, eliminates only T2 outcome (Fig. 13).

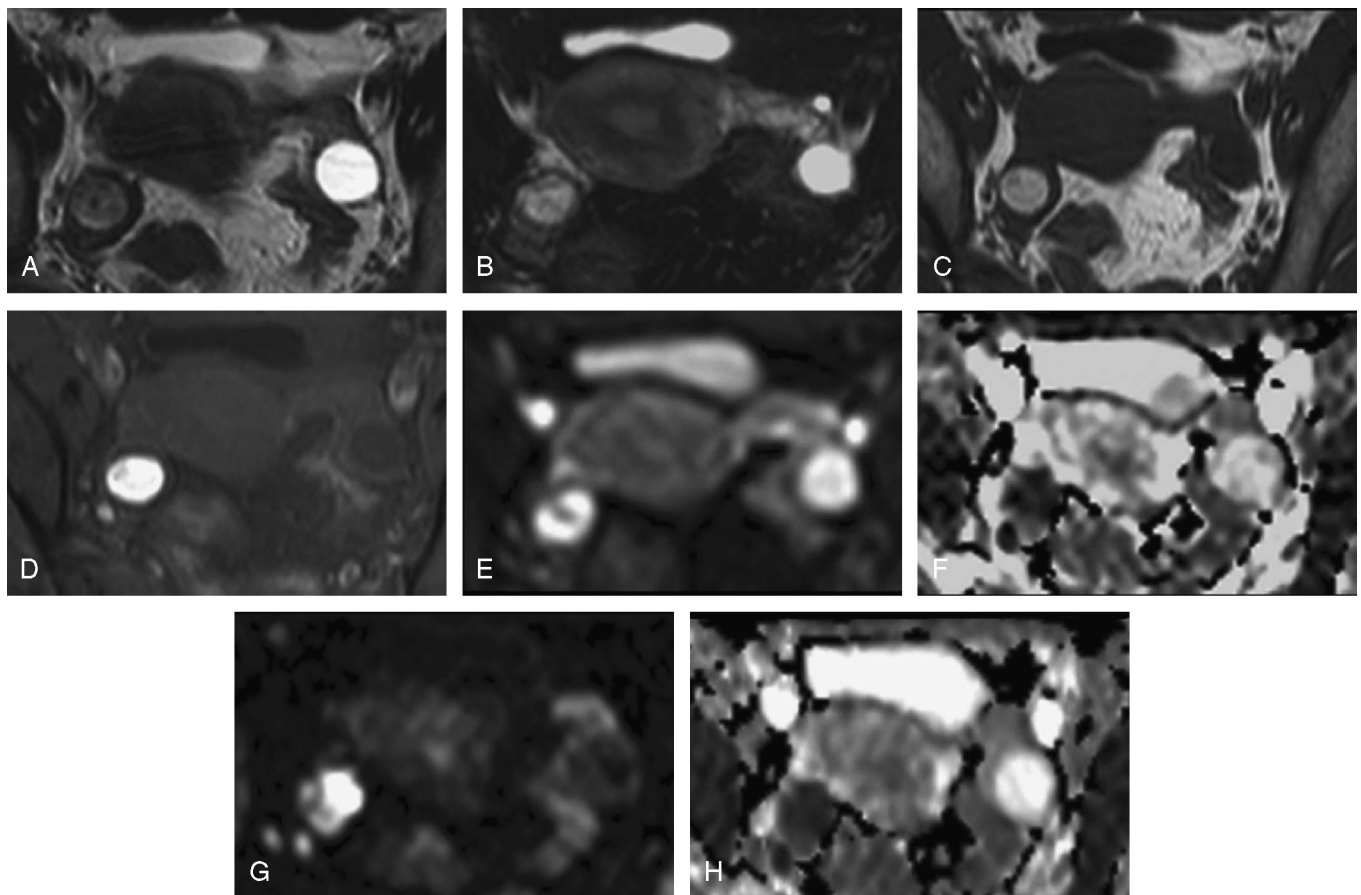


**FIGURE 7.** A 32-year-old woman with endometriosis cyst on the right ovary and simple cyst on the left ovary: shine-through effect. Axial turbo spin-echo T2-weighted (repetition time/echo time, 4800/115) without (A) and with (B) fat suppression MR images show lower SI on the right cyst due to blood debris. Axial SE T1-weighted (450/12) MR images without (C) and with (D) fat suppression, demonstrate hyperintensity of the right cyst because of presence of methemoglobin. Axial single-shot echo-planar DW MR image (1534/62), b value  $300 \text{ s/mm}^2$  (E), and corresponding ADC map (F), shows DW high SI in both the cysts because of shine-through effect, whereas ADC map demonstrates lower diffusion on the right due to blood debris. Axial single-shot echo-planar DW MR image (1714/74), b value of  $1000 \text{ s/mm}^2$  (G), and corresponding ADC map (H) confirms the same ADC map of the previous image, with different SI in DW (high on the right and low on the left side) due to the high value of b factor and subsequent lessening of shine-through effect.



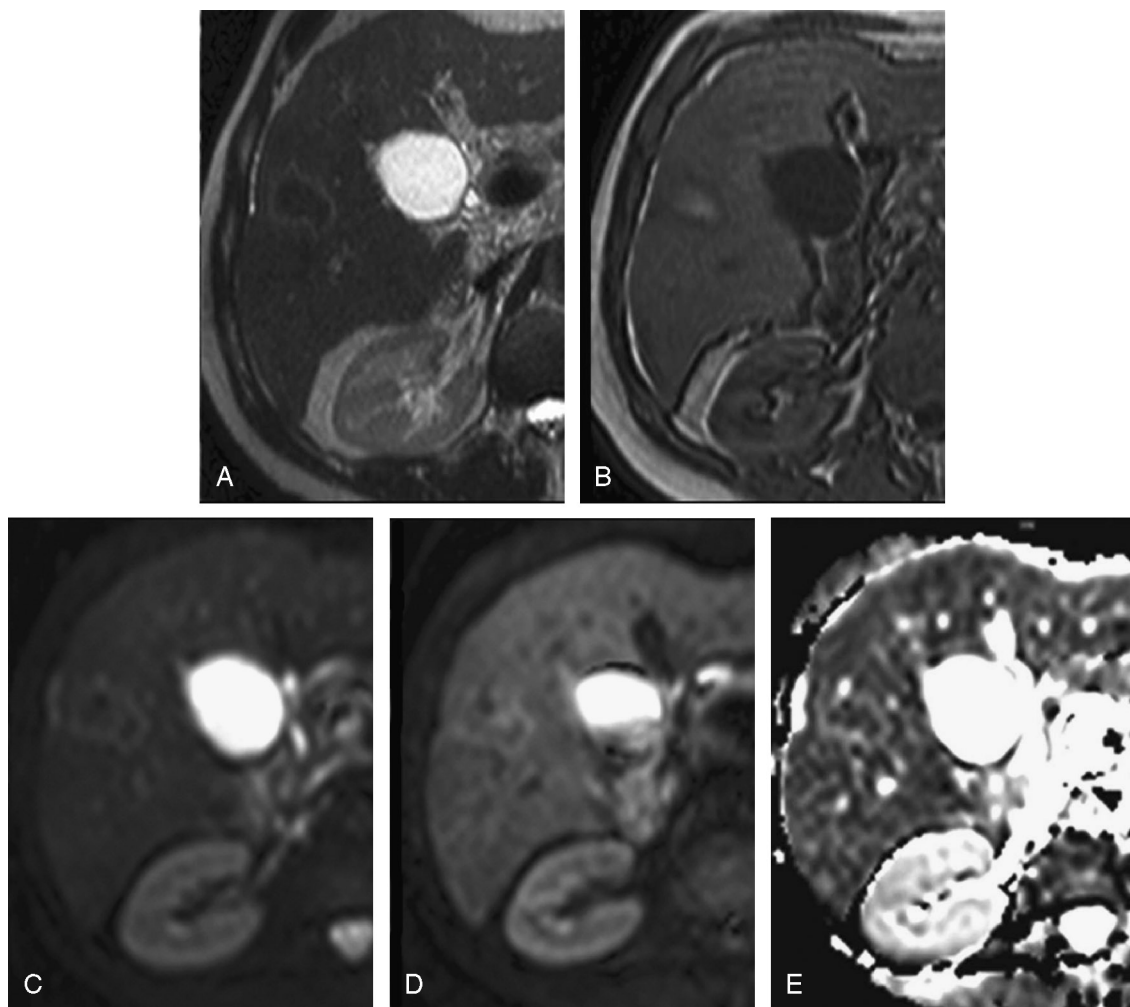


**FIGURE 8.** A 71-year-old man with coagulative necrosis area as outcome of previous treatment by radiofrequency of hepatocellular carcinoma in cirrhosis: lack of mobile spin effect. Axial T2-weighted (repetition time/echo time, 830/80) (A) and axial T1-weighted (146/2) (B) MR images show an ovoid lesion hypointense and hyperintense, respectively, surrounded by a tiny edge due to reactive edema. Axial single-shot echo-planar DW MR image (1534/62,  $b = 0 \text{ s/mm}^2$  [C],  $b = 300 \text{ s/mm}^2$  [D]) and corresponding ADC map (E) shows low SI in both isotropic DW image and ADC map. Therefore, in trace image, low SI is not due to high diffusivity, but to an absence of diffusible substrate typical of coagulative necrosis (lack of mobile spin effect).

In conclusion, in DW images acquired with a low  $b$  value ( $<500 \text{ s/mm}^2$ ), a high SI area may correspond to the following:

- truly reduced diffusivity, resulting in low ADC value (Figs. 2, 4); and
- high diffusivity with shine-through effect due to liquid content, with consequent high ADC value; shine-through effect decreases when  $b$  value increases and can be eliminated by calculating ADC maps (Figs. 4, 6 and 7).

Conversely, a low DWI SI at low  $b$  value may be the result of 3 main possibilities:

- truly high diffusivity, with elevated ADC value (Figs. 4, 6, 7);
- lack of mobile spin caused by a reduction of the diffusible substrate, with consequent low ADC rate; T2 effects can be withdrawn by calculating ADC maps (Figs. 3, 8); and

- pseudodiffusion and macroscopic motion, where the additional motion always determines elevated ADC values; pseudodiffusion effects can be lowered only by increasing the  $b$  value (Figs. 9–11).

High  $b$  values are routinely adopted in the study of the brain and of other *nonmobile* anatomical regions such as muscles, bone marrow, and joints with a significant improvement in results. However,  $b$  values higher than  $500 \text{ s/mm}^2$  are often found to produce an unacceptably low image signal in the upper abdomen. In this region, in fact, there are various sources of extremely relevant artifacts caused by cardiovascular, respiratory and peristaltic movements or by susceptibility changes at the interfaces between liver and lung. The selection of the  $b$  value should be consequently based on a compromise between image quality and adequate diffusion gradient intensity.

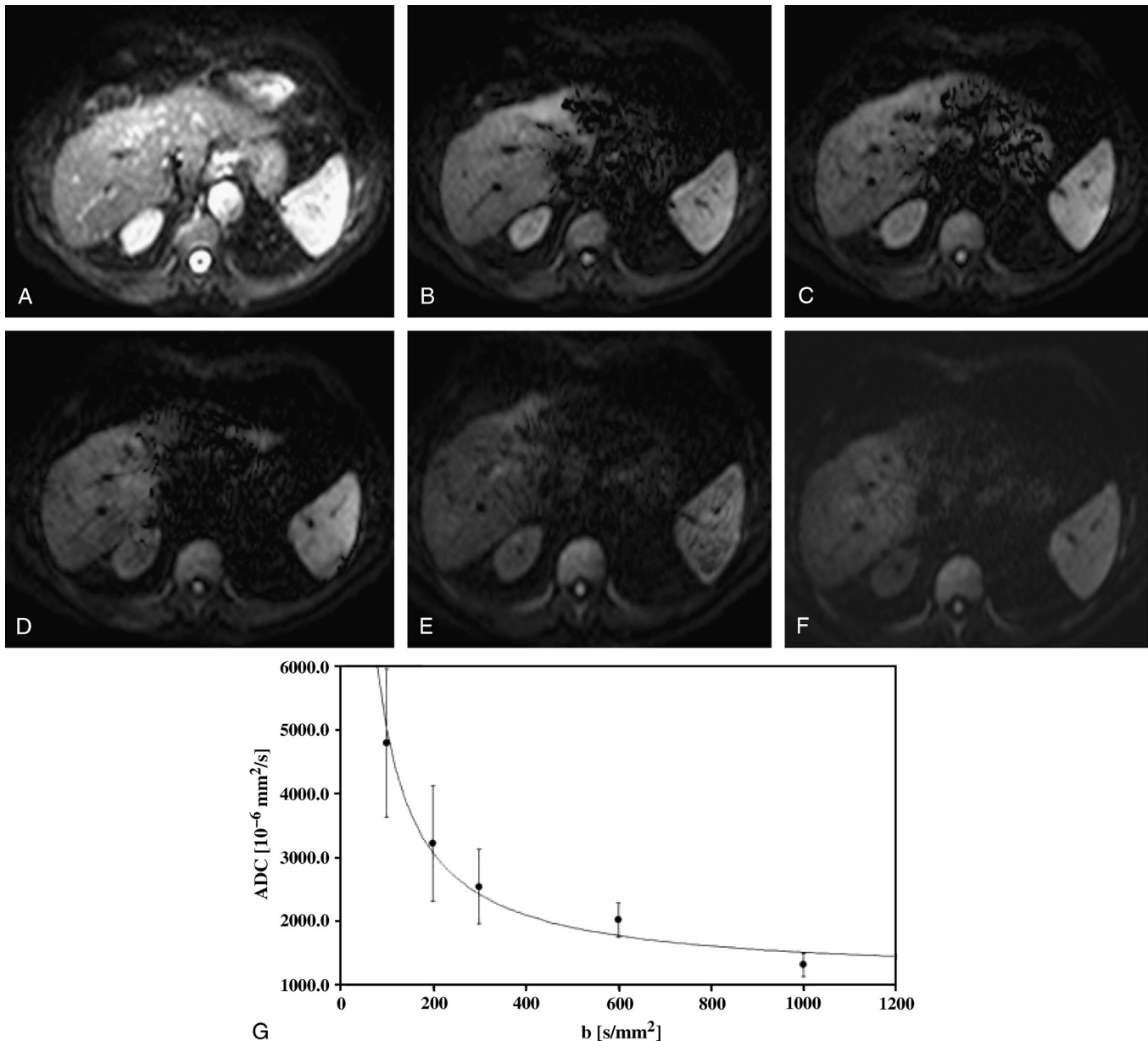


**FIGURE 9.** A 58-year-old man with liver cirrhosis: influence of b factor on pseudodiffusion effects. Axial single-shot echo-planar DW MR images (1900/74), b values 0 (A), 100 (B), 200 (C), 300 (D), 600 (E), and 1000  $\text{s}/\text{mm}^2$  (F). The ADC of a liver region of interest is plotted (y axis) (G) versus sensitization factor b (x axis) (dot points corresponding to  $b = 100, 200, 300, 600, 1000 \text{ s}/\text{mm}^2$ ). Images and graph demonstrate that the pseudodiffusion effects are lower when higher b values are used. The contribution of perfusion to ADC values decreases as b grows. According to the equation  $7b$  ( $\text{ADC} \approx D + f/b$ ), a regression curve (continuous line) is drawn through the experimental points by means a best-fit procedure taking into account the error (SD) of the SI, as well. This let us get a mathematical separation of the 2 different effects (D and  $D^*$ ) and calculate the perfusion volume fraction  $f$ . As outcome of the best-fit algorithm, it has been obtained the perfusion volume fraction  $f$  equal about to 0.39.

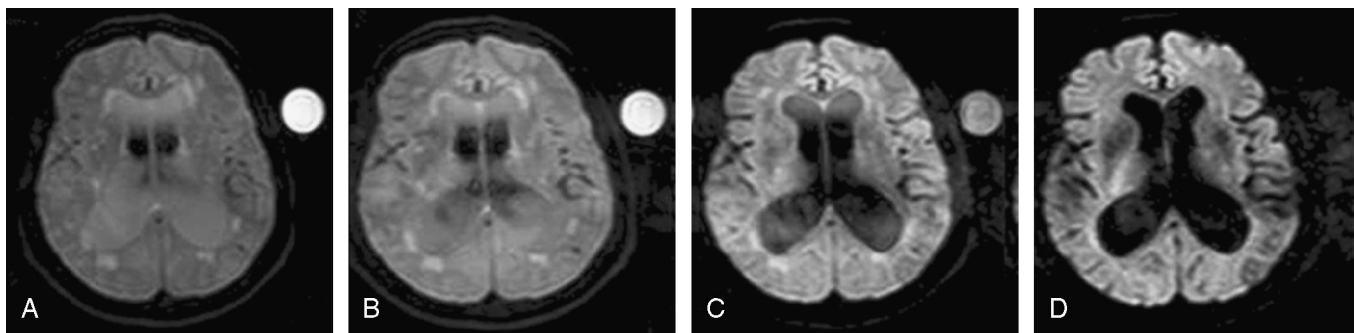


**FIGURE 10.** A 73-year-old man with normotensive hydrocephalus, with a test tube filled with saline solution on the left side of the head: influence of b factor on macroscopic motion effects. Axial nongated single-shot echo-planar DW MR images (repetition time/echo time, 2700/125), b values 150 (A), 300 (B), 600 (C), and 1200 s/mm<sup>2</sup> (D) showing, at low b values, different SI in ventricles and in the test tube not completely justified by the different temperature of the 2 areas. This difference can be explained by CSF flow. In the test tube solution, there is not an additional water dislocation because of CSF dislocation. By increasing the b value from 150 to 1200 s/mm<sup>2</sup>, this difference in SI progressively reduces, without dissolving completely, as confirmed by ADC calculation (see also Figs. 11, 12).

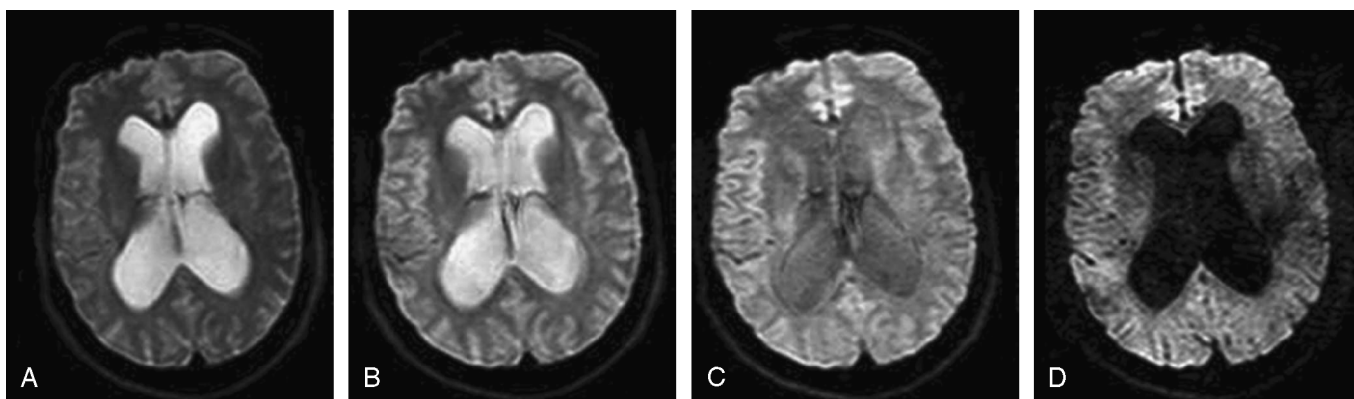


**FIGURE 11.** A 62-year-old man with obstructive hydrocephalus: influence of b factor on macroscopic motion effects. Axial nongated single-shot echo-planar DW MR images (repetition time/echo time, 2700/125) and b values 150 (A), 300 (B), 600 (C), and 1200 s/mm<sup>2</sup> (D) show an increase in DW SI, when CSF flow decreases, as in the case of obstructive hydrocephalus (confirmed by ADC calculation). The given example shows that for low b factor intensity, macroscopic motion markedly influences ADC values. On the contrary, high b values (>1000 s/mm<sup>2</sup>) almost completely eliminate the effects induced by macroscopic motion (see also Figs. 10, 12).

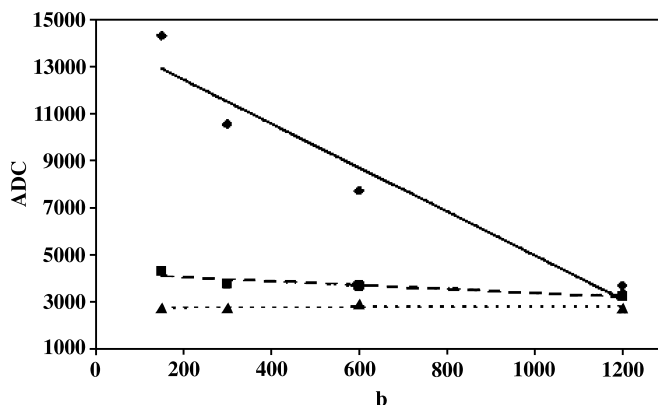


**FIGURE 12.** Graph: influence of b factor on macroscopic motion effects (referred to Figs. 10, 11). The ADC (y axis) calculated in ventricles of normotensive hydrocephalus (♦), obstructive hydrocephalus (■), and test tube containing saline solution (▲) are plotted versus the b factor values (x axis). Three regression lines are drawn through the experimental points. As demonstrated, at low b factor values, macroscopic motion markedly influences ADC calculation. In fact the ADC of normotensive hydrocephalus is much higher than that of obstructive hydrocephalus. On the contrary, high b values lower the effects induced by macroscopic motion especially for normotensive hydrocephalus, whereas become almost negligible for obstructive hydrocephalus. Finally, the higher ADC of CSF with respect to saline solution at b equals to 1200 s/mm<sup>2</sup>, is explained by the different temperatures (37° and 22°, respectively).

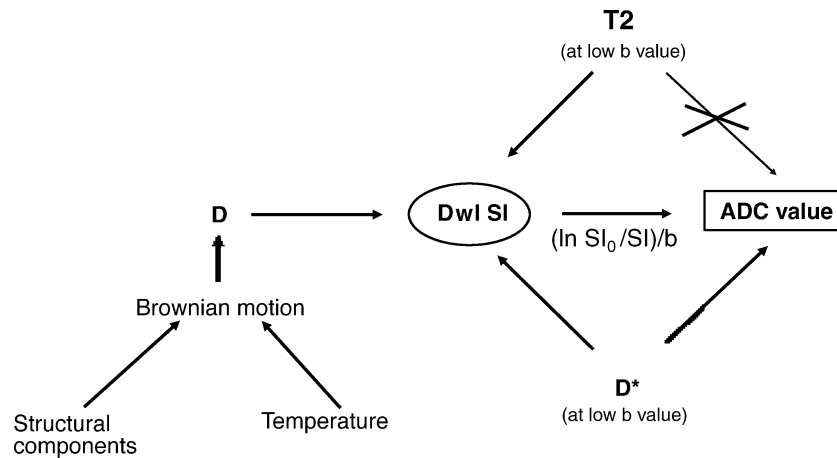


**FIGURE 13.** Relationship among diffusivity, DWI SI, ADC value, and main connected factors. In DWI, SI is mainly influenced by diffusivity, pseudodiffusion, and T2 intensity value; the latter is to be considered an index of the amount of free-water molecules. Apparent diffusion coefficient is a scalar quantity parameter incorporating all the IVIM, but insensitive to T2 effects.

### ACKNOWLEDGMENT

The authors thank Dr Catherine Arcella for the careful revision of the paper.

### REFERENCES

1. Stejskal EO, Tanner JE. Spin diffusion measurements: spin echoes in the presence of time-dependent field gradient. *J Chem Phys.* 1965;42: 288–292.
2. Carr HY, Purcell EM. Effects of diffusion on free precession in nuclear magnetic resonance experiments. *Phys Rev.* 1954;94:630–638.
3. Thomas DL, Lythgoe MF, Pell GS, et al. The measurement of diffusion and perfusion in biological systems using magnetic resonance imaging. *Phys Med Biol.* 2000;45:97–138.
4. Cercignani M, Horsfield MA. The physical basis of diffusion-weighted MR. *J Neurol Sci.* 2001;186:11–14.
5. Yamada I, Aung W, Himeno Y, et al. Diffusion coefficients in abdominal organs and hepatic lesions: evaluation with intravoxel incoherent motion echo-planar MR imaging. *Radiology.* 1999;210: 617–623.
6. Schaefer PW, Grant PE, Gonzalez RG. Diffusion-weighted MR imaging of the brain. *Radiology.* 2000;217:331–345.
7. Colagrande S, Pallotta S, Vanzulli A, et al. The diffusion parameter in magnetic resonance: physics, techniques, and semeiotics. *Radiologia Medica.* 2005;109:1–16.
8. Pierpaoli C, Jezzard P, Basser PJ, et al. Diffusion tensor MR imaging of the human brain. *Radiology.* 1996;201:637–648.
9. Burdette JH, Elster AD, Ricci PE. Acute cerebral infarction: quantification of spin-density and T2 shine-through phenomena on diffusion-weighted MR images. *Radiology.* 1999;212: 333–339.
10. Le Bihan D, Breton E, Lallemand D, et al. Separation of diffusion and perfusion in intravoxel incoherent motion MR imaging. *Radiology.* 1988;168:497–505.